Modelling Uranyl Chemistry in Liquid Ammonia from Density Functional Theory.

Nicolas Sieffert, Amol Thakkar, and Michael Bühl *

-- Electronic Supporting Information --

Full computational Details

I. Static calculations

Geometries and thermodynamic corrections. Geometries of all complexes were fully optimized at the B3LYP-D3(bj)/SDD/6-311+G(d,p) level, i.e. employing the B3LYP[1] functional including the latest version of the Grimme's "-D3" dispersion correction,[2] in conjunction with the SDD basis on U, denoting the small-core Stuttgart–Dresden relativistic effective core potential (ECP) together with its valence basis set,[3] and the standard 6-311+G(d,p)[4] basis for all other elements. Harmonic frequencies were computed analytically and were used without scaling to obtain enthalpic and entropic corrections at T = 298.15 K and P = 1 atm. The corresponding correction terms δE_G were estimated at the same SDD/6-311+G(d,p) level and have been obtained as the difference of the reaction energy of a given step (ΔE) and the corresponding free energy (ΔG):

$$\delta E_G = \Delta G - \Delta E \qquad \text{(eq. 5)}$$

The initial structures of the complexes were constructed by hand and were derived from our previous study.[5]

Refined energies for the calculation of ΔE_{gas} and δE_{BSSE}. Refined energies were obtained from single-point calculations (on the B3LYP-D3(bj)/SDD/6-311+G(d,p) geometries) using the same SDD ECP on U and the larger cc-pVTZ[6] basis sets on all elements.

The following functionals have been tested: ωB97,[7] ωB97X,[7] PBE0-D3(bj),[2, 8] PBE0, B3LYP-D3(bj), B3LYP,[1] B3PW91,[1a, 9] B3PW91-D3(bj), BLYP,[1b, 10] BLYP-D3(bj), BP86,[10-11] BP86-D3(bj), B97-D3(bj),[2, 12] M05-2X,[13] M06,[14] M06-2X[14] and M06-L.[15]

Refined reaction energies computed with these functionals are gathered in Table S1.

The basis set superposition error (BSSE) have been calculated using the counterpoise method.[16] For eq. 2 and 3, the NH_3 ligand involved in the dissociation/association reaction is defined as the first fragment and the rest of the complex is the second fragment. Similarly, for eq. 4, the two dissociated NH_3 ligands are defined as the first fragment and the rest of the complex is the second fragment in compounds **3'**, **4'** and **5'**. In complex **3**, **4** and **5**, the two halides constitute the first fragment and the second fragment is the rest of the complex. The BSSE energy corrections (noted δE_{BSSE}) are gathered in Tables 3 and S2-S3.

Because BSSE is nearly identical at the MP2 and CCSD(T) levels (see Table S3), δE_{BSSE} have been computed at the former level to correct our two reference calculations. Also, BSSE is not critically dependant to the employed DFT method, so that BSSE corrections computed with the PBE0 functional have been applied at all DFT/SDD/cc-pVTZ levels.

Correcting term for solvation effects (δE_{solv}). The δE_{solv} energy correction is defined as the difference between the reaction energy in the continuum (ΔE_{CSM}) and in the gas phase (ΔE_{gas}):

$$\delta E_{solv} = \Delta E_{CSM} - \Delta E_{gas} \qquad \text{(eq. 6)}$$

Unless otherwise specified, ΔE_{gas} and ΔE_{CSM} have been computed from single points at the B3LYP/SDD/6-311+G** level on the gas phase optimized geometries (B3LYP-D3(bj)/SDD/6-311+G**). Other combinations of functionals and basis sets have been investigated (see Table 2). We also investigated the effect of the geometry, by considering CSM-optimized geometries to compute ΔE_{CSM} (IEFPCM/UA0 model, *vide infra*) and gas phase optimized geometries to compute ΔE_{gas}. These calculations have all been performed using the BLYP functional (see Table 2).

The IEFPCM,[17] CPCM,[18] IPCM[19] and SMD[20] models, from Gaussian09,[21] have been investigated. The COSMO[22] model, as implemented in the Turbomole package,[23] has also been considered. The "UFF" cavity model uses radii from the UFF[24] force field and hydrogens have individual spheres (explicit hydrogens). UA0 and UAKS uses the United Atom Topological Model (hydrogens are enclosed in the sphere of the heavy atom to which they are bonded), applied on atomic radii of the UFF force field for heavy atoms (UA0), or

applied on radii optimized for the PBE1PBE/6-31G(d) level of theory (UAKS). Note that the non-electrostatic terms have not been included in our IEFPCM and CPCM calculations.
The standard isodensity value of 0.001 a.u. has been employed in IPCM calculations.
The dielectric constant was 16.6 to describe liquid ammonia throughout.
The following element radii were used in all COSMO calculations: U 2.22 Å, O 1.72 Å, N 1.83 Å, and H 1.30 Å. The default value of rsolv (1.3000 Å) has been used. All COSMO calculations included the outlying charge correction.[25] These calculations were performed with the Turbomole package (version 6.4).[23]

As for the SMD model, the following input parameters has been used:

Eps=16.6	ε
EpsInf=1.776089	n^2
HbondAcidity=0.14	α
HbondBasicity=0.62	β
SurfaceTensionAtInterface=29.00	γ
CarbonAromaticity=0.	ϕ
ElectronegativeHalogenicity=0.	ψ

EpsInf ($=(n_D^{20})^2$) has been obtained from $n_D^{20} = 1.3327$ at 20°C.[26]
$\alpha = 0.14$ and $\beta = 0.62$ were taken from Reference [27], consistently to the parameterisation of several alkylamines from the SMD database.[20]
Surface tension of liquid ammonia is 23.38 dynes/cm at 11.10°C and 18.05 dynes/cm at 34.05°C.[28] Linear interpolation provides a surface tension of 20.15 dynes/cm at 25°C. After applying the conversion factor (1 dyn/cm = 1.43932 $cal.mol^{-1}.A^{-2}$), a surface tension value of 29.00 is obtained.

Results of the benchmarking of these implicit solvation models are given in Tables 2 and S4.

Final reaction free energies in solution. The final ΔG_{liq} values are calculated as a sum of all energy correction terms, added to the raw gas phase reaction energies (ΔE_{gas}):

$$\Delta G_{liq} = \Delta E_{gas} + \delta E_{solv} + \delta E_{BSSE} + \delta E_G. \qquad \text{(eq. 1)}$$

II. Car-Parrinello Molecular Dynamics (CPMD) calculations.

CPMD[29] simulations were performed using the exact same parameters as those employed in reference [5]. Namely, the BLYP,[1b, 10] functional has been employed, alongside norm-conserving pseudopotentials that had been generated according to the Troullier and Martins procedure[30] and transformed into the Kleinman-Bylander form.[31] Kohn-Sham orbitals were expanded in plane waves at the Γ-point up to a kinetic energy cutoff of 80 Ry. A fictitious electronic mass of 600 a.u. and a time step of 0.121 fs have been employed. All hydrogen atoms have been replaced by Deuterium. The simulated system (in explicit ammonia) consists on one complex **1** and 37 NH_3 molecules, in a (periodic) cubic box with box size of 13.22 Å. The simulations was restarted from the previously equilibrated system described in reference [5]. For CPMD calculations in vacuum, the simulated systems consisted on a single complex in a (periodic) cubic box of cell length 13.22 Å. "CP-opt" denotes geometry optimizations at the Car-Parrinello level, using the exact same parameters as in CPMD simulations in vacuum. Structures were optimized until the maximum gradient was less than 5.10^{-4} a.u.
These simulations were performed with the CPMD program.[29b]

Pointwise integration (PTI) calculations in solution.

Constrained CPMD simulations were performed along a predefined reaction coordinate ξ (the difference between two U-N distances, see Scheme S1), starting from the respective mean values for the five-coordinate minumum in solution (as obtained from the unconstrained simulation from reference [5]). Changes in the Helmholtz free energies were evaluated by pointwise thermodynamic integration[32] of the mean constraint force ⟨f⟩ along this coordinate via:

$$\Delta A_{\mathrm{a}\rightarrow\mathrm{b}} = -\int_{\mathrm{a}}^{\mathrm{b}} \langle f(\xi) \rangle \mathrm{d}\xi$$

At each point, the system was propagated until ⟨f(ξ)⟩ was sufficiently converged (usually within 2-2.5 ps after 0.5 ps of equilibration. Each new point was continued from the final, equilibrated configuration of the previous one, using 2000 steps of continuous slow growth to increase the constrained distances.

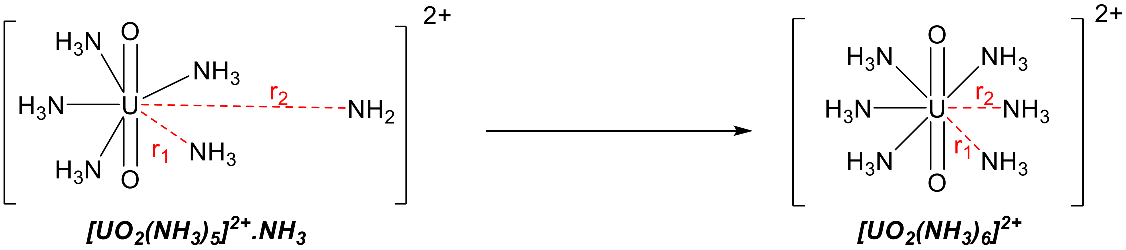

Scheme S1: Association of an ammonia ligand from the second coordination sphere to form the $[UO_2(NH3)_6]^{2+}$ species, where the reaction coordinate is given as the difference $\Delta r = r_1 - r_2$ shown in red.

PTI calculations in the gas phase.

Simulation times were 2-3 ps after 0.5 ps of equilibration for the gas phase. The largest standard deviation for the running average of <f(ζ)> over the final picosecond of any point was 7.9 x 10^{-4} a.u in the gas phase multiplied by the total integration width 2.6 Å in the gas phase, this corresponds to an estimated numerical uncertainty of *ca*. 2.4 kcal mol^{-1} for the derived energy values. Each subsequent point was started from the final, equilibrated configuration of the previous one.

The values for ζ (the constrained differences of U-N distances, in Å) and <f(ζ)> (the mean force, in a.u.), for eq.3 in the gas phase are:

ζ	<f(ζ)>[a]
0.0000	0.00009(7)
0.2000	-0.00179(36)
0.4000	-0.00183(42)
0.5000	-0.00035(8)
0.6000	0.00138(26)
0.8000	0.00415(17)
1.0000	0.00360(4)
1.2000	0.00327(4)
1.4000	0.00228(3)
1.6000	0.00168(8)
1.8000	0.00189(8)
2.0000	0.00117(6)
2.2000	0.00046(5)
2.4000	-0.00075(5)
2.6000	-0.00149(9)

[a] In parentheses: standard deviation of the running average of <f(ζ)> over the last picosencond.

When Δr approaches zero, unconstrained ammine ligands tend to drift off. Where this has occurred a further constraint has been implemented, such that the difference between two additional bond lengths has been held constant (see Scheme S2). Notably, this was implemented between Δr = 0 and -0.4 Å. As a pre-defined reaction coordinate has been used, only the upper limit to the barrier can be obtained.

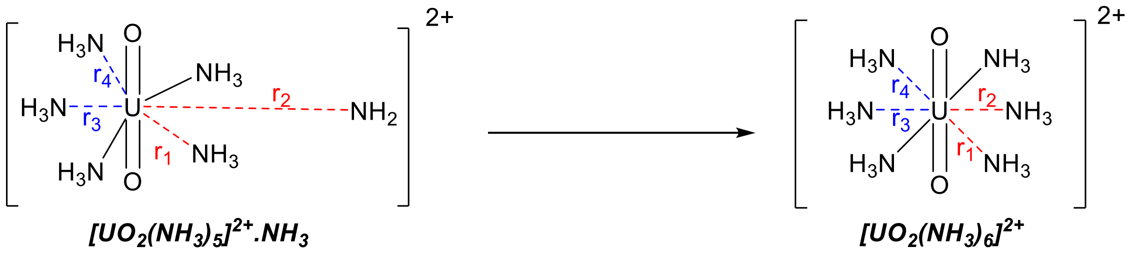

Scheme S2: Association of an ammonia ligand from the second coordination sphere to form the $[UO_2(NH_3)_6]^{2+}$ species, where the reaction coordinate is given as the difference $\Delta r = r_1 - r_2$ shown in red. The additional constraint is given as the difference $\Delta r = r_3 - r_4$ shown in blue.

III Thermochemistry correction: comparison between "static" DFT calculations (G09) and (gas-phase) CPMD simulations.

The values of the thermochemistry correcting term (namely δE_G), estimated from static DFT calculations, can be compared to CPMD results in the gas phase by calculating the difference between reaction free energies computed from PTI technique (ΔA(gas,CPMD)) and the reaction energies, obtained from gas-phase optimization at the CP-opt level (namely, DE(gas,CP-opt), see section I and II below for details). However, because CPMD simulations are based on classic equations of motion for the nuclei, the zero-point energy (ZPE) is not accounted for in CPMD results. The thermochemistry correction $\delta E'_G$ without ZPE can be computed as follows:

$$\delta E'_G \text{ (CPMD)} = (\Delta A(\text{gas,CPMD})) - \Delta E(\text{gas,CP-opt}) \quad \text{(eq. 7)}$$

The latter can be computed at the static B3LYP-D3(bj)/SDD/6-311+G** level:

$$\delta E'_G \text{ (Static)} = (\Delta G - \Delta ZPE) - \Delta E = \delta E_G - \Delta ZPE \quad \text{(eq. 8)}$$

where ΔZPE stands for the correction for zero point energies. Note that the latter is small, namely -0.9 and +0.8 kcal/mol for eq. 2 and 3, respectively (see Table S5). Interestingly, static calculations allow for a good estimate of the thermochemistry corrections, as they provide $\delta E'_G$ values in good agreement with CPMD results for eq. 3 (within 0.2 kcal/mol), whereas a larger deviation is found for eq. 2 (within 2.7 see Table S5).

Table S5: Calculation of the correcting term for thermochemistry (namely, $\delta E'_G$, in kcal/mol) based either on CPMD simulations or static G09 calculations.

	CPMD			**Static (G09)**		
	ΔA_{gas}	ΔE_{gas}	$\delta E'_G$ [a]	δE_G	ΔZPE	$\delta E'_G$ [b]
Eq. 2	5.4	8.0	-2.6	-0.8	-0.9	0.1
Eq. 3	6.6	3.7	2.9	3.5	0.8	2.7

a. Computed according to eq. 7. *b.* according to eq. 8.

Additional Tables S1-S4.

Table S1: Influence of the density functional on the reaction energies corresponding to eq. **2**, and **3**. Raw reaction energies, without correction for BSSE.[a]

	ΔE Eq. 2	**ΔE Eq. 3**
CCSD(T)/cc-pVTZ	11.0	6.1
BLYP	4.8	6.8
BLYP-D3(bj)	8.2	3.6
B3LYP	7.7	7.6
B3LYP-D3(bj)	10.5	4.9
PBE0	8.6	7.0
PBE0-D3(bj)	9.9	5.8
B3PW91	7.3	7.7
B3PW91-D3(bj)	10.1	5.1
BP86	5.0	6.4
BP86-D3(bj)	7.7	3.8
M06	12.4	4.0
M06-L	11.8	0.7
M06-2X	15.2	5.0
M05-2X	14.9	5.1
APF	8.1	7.3
B97-D3(bj)	7.2	4.3
ωB97	12.3	6.5
ωB97X	11.4	6.9

*a.*The same SDD/cc-pVTZ basis set has been employed throughout.

Table S2: BSSE (kcal/mol) obtained at different computational levels and with different basis sets for eq. 2.[a]

Level	**Basis set**	**Complex 1 BSSE**	**Complex 1' BSSE**	**δE_{BSSE}**
PBE0	cc-pVTZ	1.6	1.3	-0.3
MP2	cc-pVTZ	2.9	1.9	-1.0

a The counterpoise method has been employed using two fragments: the first fragment is the dissociated NH_3 ligand, and the second is the rest of the complex.

Table S3: BSSE (kcal/mol) obtained at different computational levels and with different basis sets for eq. 3.[a]

Level	**Basis set**	**Complex 2' BSSE**	**Complex 2 BSSE**	**δE_{BSSE}**
HF	cc-pVDZ	2.3	3.6	1.3
MP2	cc-pVDZ	4.1	8.0	3.9
CCSD(T)	cc-pVDZ	4.1	8.0	3.9
HF	cc-pVTZ	0.9	2.4	1.5
PBE0	cc-pVTZ	1.3	1.7	0.4
MP2	cc-pVTZ	1.9	3.1	1.2
CCSD(T)	cc-pVTZ	1.8	3.1	1.3

a The counterpoise method has been employed using two fragments: the first fragment is the associated NH_3 ligand, and the second is the rest of the complex.

Table S4: Correcting term for solvation effects (δE_{solv}, in kcal/mol) computed using different implicit and explicit solvent models, and using different combination of basis set and density functionals.

	Basis set	**Functional** [a]	**δE_{solv}** [b] **(eq. 2)** ***dissoc.***	**δE_{solv}** [b] **(eq. 3)** ***assoc.***
CPMD (explicit solvent)			3.8	-1.1
	*B3LYP-D3(bj)/SDD/6-311+G** optimized structures in vacuum.* [c]			
IEFPCM/UFF	SDD/6-311+G**	B3LYP	0.8	-3.9
CPCM/UFF	SDD/6-311+G**	B3LYP	0.1	-4.0
IEFPCM/UA0	SDD/6-311+G**	B3LYP	5.5	-5.1
CPCM/UA0	SDD/6-311+G**	B3LYP	5.6	-5.2
IEFPCM/UAKS	SDD/6-311+G**	B3LYP	3.6	-6.2
CPCM/UAKS	SDD/6-311+G**	B3LYP	3.4	-6.8
IPCM	SDD/6-311+G**	B3LYP	8.1	-5.2
COSMO	SDD/6-311+G**	B3LYP	5.7	-3.7
COSMO	SDD/cc-pVTZ	B3LYP	5.6	-3.6
COSMO	SDD/cc-pVTZ	BLYP	5.6	-3.9
SMD	SDD/6-311+G**	B3LYP	2.2	-5.1
SMD	SDD/cc-pVTZ	B3LYP	2.3	-5.1
SMD	SDD/cc-pVTZ	M06-2X	2.0	-4.7
SMD	SDD+/aug-cc-pVTZ	M06-2X	1.9	-4.6
	*BLYP/SDD/6-311+G** optimized structures in the continuum.* [d]			
IEFPCM/UFF	SDD/6-311+G**	BLYP	-0.1	-4.2
CPCM/UFF	SDD/6-311+G**	BLYP	-0.5	-4.2
IEFPCM/UA0	SDD/6-311+G**	BLYP	5.4	-5.5
CPCM/UA0	SDD/6-311+G**	BLYP	5.5	-5.6
IEFPCM/UAKS	SDD/6-311+G**	BLYP	3.5	-7.7
CPCM/UAKS	SDD/6-311+G**	BLYP	3.4	-7.8
IPCM	SDD/6-311+G**	BLYP	3.6	-4.5
COSMO	SDD/6-311+G**	BLYP	5.1	-4.5
COSMO	SDD+/aug-cc-pVTZ	BLYP	4.9	-4.3
SMD	SDD/6-311+G**	BLYP	2.1	-6.1

a. Functional employed to perform the single point energy calculations, both in the gas phase (to compute ΔE_{gas}) and in the continuum (to compute ΔE_{solv}). *b.* $\delta E_{solv} = \Delta E_{solv} - \Delta E_{gas}$. *c. Single points on gas phase B3LYP-D3(bj)/SDD/6-311+G** optimized structures. d. Single points on BLYP/SDD/6-311+G** optimized structures, considering gas phase optimized structures for ΔE_{gas} and IEFPCM/UA0 optimized structures for ΔE_{solv}.*

```
XYZ Coordinates (in A):
Optimized geometries at the B3LYP-D3(bj)/SDD/6-311+G** level.

   23
```

Complex 1

```
U     0.000091    -0.004334    -0.000961
O     0.005875    -0.003719     1.752695
O     0.008380    -0.006111    -1.754686
N     2.590387     0.418879     0.030889
N     0.413301     2.583233    -0.164315
N    -2.318782     1.208366     0.224190
N    -1.880918    -1.824531    -0.209122
N     1.179210    -2.346734     0.105154
H     2.961780     0.692164    -0.880418
H     2.860920     1.155813     0.683751
H     3.152550    -0.383692     0.314476
H    -0.312940     3.057851    -0.702302
H     0.461586     3.069164     0.732712
H     1.275941     2.822884    -0.654059
H    -2.798986     1.419149    -0.652191
H    -2.979375     0.667098     0.783583
H    -2.248973     2.096383     0.722577
H    -1.619439    -2.566796    -0.859564
H    -2.143269    -2.288264     0.662240
H    -2.750778    -1.457766    -0.596948
H     1.733076    -2.570694    -0.723206
H     1.810611    -2.420453     0.904179
H     0.543661    -3.136646     0.218937
```

```
   23
```

Complex 1′

```
U    -0.327383     0.165613    -0.007810
O    -0.295951     0.303496    -1.754318
O    -0.364935     0.026658     1.738549
N     1.871462     1.413408     0.136275
N     1.289328    -1.786313    -0.129728
N     4.192024    -0.639238     0.051657
N    -2.402481    -1.364969    -0.159781
N    -1.698846     2.349247     0.126797
H     2.645451     0.721446     0.109573
H     2.048840     2.057370    -0.636195
H     2.003184     1.944804     0.998407
H     1.210509    -2.458586     0.634875
H     1.248412    -2.322255    -0.998030
H     2.252008    -1.407851    -0.074753
H     4.471973    -1.207144     0.851795
H     4.517361    -1.146777    -0.771579
H     4.799361     0.179696     0.097760
H    -3.121913    -1.146273     0.533136
H    -2.864129    -1.340221    -1.071197
H    -2.181863    -2.350347     0.004061
H    -2.013341     2.576189     1.072219
H    -1.177546     3.168284    -0.195024
H    -2.538809     2.339363    -0.456587
```

```
   27
```

Complex 2

U	-0.001843	-0.001800	0.000307
O	-0.003819	-0.004730	-1.763177
O	-0.004464	-0.003031	1.763782
N	-2.548883	-0.467391	-0.657866
N	2.541609	0.471184	0.673940
N	0.867457	2.435485	-0.673782
N	-1.676659	1.973920	0.665621
N	-0.865875	-2.444406	0.657437
N	1.683934	-1.967181	-0.665196
H	2.871213	-0.283964	1.274852
H	3.266448	0.603512	-0.030806
H	1.688520	2.341055	-1.271282
H	0.173730	2.880640	-1.274320
H	2.163176	-2.523435	0.042358
H	2.416613	-1.587541	-1.264489
H	-2.150972	2.534308	-0.042005
H	-1.185402	2.638192	1.263534
H	-1.687948	-2.358048	1.254753
H	-0.171795	-2.893967	1.254241
H	-3.267298	-0.597955	0.053758
H	-2.593968	-1.293008	-1.254712
H	-2.881799	0.289265	-1.255013
H	1.113876	3.130950	0.030002
H	2.578804	1.297397	1.270577
H	1.197205	-2.635428	-1.262357
H	-1.109338	-3.133060	-0.054014
H	-2.412573	1.599142	1.263959

27

Complex 2′

U	-0.272887	0.000205	-0.024692
O	-0.476543	0.000156	-1.769271
O	-0.073653	0.000386	1.720627
N	4.454715	-0.001218	0.300840
N	1.794541	-1.538612	-0.211972
N	1.795364	1.537930	-0.212951
N	-1.129314	2.486916	-0.077516
N	-2.864051	0.000934	0.463726
N	-1.130957	-2.485967	-0.077789
H	2.668970	-1.013347	-0.048335
H	1.805670	-2.294464	0.472732
H	1.807099	2.294351	0.471100
H	2.669382	1.012169	-0.049099
H	-2.041312	-2.583858	-0.528189
H	-1.219064	-2.927909	0.838248
H	-2.041294	2.584949	-0.524550
H	-0.518093	3.094786	-0.622826
H	-3.155431	0.804276	1.021205
H	-3.155946	-0.803253	1.019705
H	4.961473	0.797664	-0.080563
H	4.958556	-0.812359	-0.057893
H	4.645529	0.012186	1.302611
H	1.902749	1.972579	-1.129757
H	1.901978	-1.974110	-1.128377
H	-0.518111	-3.094800	-0.620194
H	-3.463187	0.001842	-0.362926
H	-1.213793	2.929679	0.838461

25

Complex 3

U	0.000015	0.373877	-0.029190
O	-0.001399	0.453543	-1.803412
N	0.002272	3.054831	0.104368
N	-2.360860	1.297390	-0.003947
N	1.482876	-1.679695	-0.083239
H	-2.612047	1.841222	-0.826642
H	-3.077906	0.451124	0.010907
H	-2.595070	1.862424	0.809211
H	1.363503	-2.239121	-0.924111
H	2.520593	-1.385218	-0.049595
H	1.332054	-2.301938	0.706864
O	0.001565	0.354004	1.746836
N	2.361180	1.297033	-0.008162
N	-1.483236	-1.679464	-0.080903
H	2.596822	1.863384	0.803653
H	3.077983	0.450553	0.007053
H	2.611538	1.839479	-0.832017
H	-1.332035	-2.301280	0.709465
H	-2.520876	-1.384737	-0.046751
H	-1.364552	-2.239405	-0.921528
F	3.843640	-0.716123	0.007034
F	-3.843748	-0.715472	0.010628
H	-0.822303	3.475722	-0.313517
H	0.813040	3.474452	-0.340956
H	0.018801	3.333979	1.082551

25

Complex 3'

U	-0.065123	-0.184710	0.155935
O	-0.267627	-1.197651	-1.309388
N	1.089787	-2.309628	1.286735
F	2.145632	-0.195766	-0.083066
F	-2.000801	0.781731	-0.234585
O	0.130358	0.710356	1.696075
N	-1.962950	-1.584669	1.314575
N	0.466628	1.931809	-1.205366
H	-2.438387	-0.941389	1.941908
H	-2.618223	-1.800250	0.544416
H	-1.773362	-2.436565	1.832104
H	-0.374379	2.496851	-1.276050
H	1.202652	2.451471	-0.703455
H	0.798857	1.729664	-2.143320
N	-3.439796	-1.558509	-1.237155
N	2.652106	2.593665	0.669369
H	0.860972	-3.222894	0.907350
H	1.093617	-2.370938	2.299890
H	2.027957	-2.058827	0.977627
H	-2.749373	-1.890593	-1.904479
H	-4.362128	-1.709640	-1.630711
H	-3.280678	-0.555301	-1.137101
H	2.880015	1.614275	0.493369
H	2.183339	2.625976	1.570061
H	3.511793	3.126713	0.741388

25

Complex 4

U	-0.000079	0.389351	-0.029812
O	-0.001810	0.473472	-1.800328
N	0.002400	3.069842	0.101573
N	-2.374622	1.320504	-0.001678
N	1.477549	-1.672381	-0.093075
H	-2.625289	1.854275	-0.831998
H	-3.106613	0.548125	0.030788
H	-2.597622	1.901356	0.804325
H	1.360566	-2.224747	-0.940201
H	2.511775	-1.452482	-0.051073
H	1.316760	-2.302649	0.690040
O	0.001772	0.365340	1.742194
N	2.374809	1.320200	-0.007025
N	-1.477951	-1.672207	-0.089577
H	2.599095	1.904034	0.796448
H	3.106601	0.547689	0.027585
H	2.624787	1.850881	-0.839525
H	-1.317779	-2.300689	0.695104
H	-2.512246	-1.452191	-0.048992
H	-1.360306	-2.226503	-0.935348
Cl	4.435326	-0.905524	0.052172
Cl	-4.435697	-0.904990	0.051436
H	-0.819293	3.496219	-0.318082
H	0.809497	3.494038	-0.347640
H	0.020218	3.359601	1.077288

25

Complex 4'

U	0.003941	-0.168614	0.102737
O	-0.425965	-1.064366	-1.373448
N	0.877610	-2.488876	1.032950
Cl	2.662991	-0.416111	-0.457547
Cl	-2.258893	1.303185	-0.111811
O	0.418093	0.605953	1.649700
N	-1.911566	-1.408817	1.375464
N	0.673226	1.907610	-1.230300
H	-2.406736	-0.679572	1.882508
H	-2.557892	-1.757390	0.646413
H	-1.712222	-2.159424	2.029249
H	-0.141282	2.464375	-1.471733
H	1.310372	2.464666	-0.637381
H	1.172336	1.660351	-2.079668
N	-3.452414	-1.813741	-1.107717
N	2.566268	2.818667	0.850893
H	0.349150	-3.309676	0.752751
H	1.013732	-2.519603	2.039199
H	1.797834	-2.535289	0.598155
H	-2.688417	-1.977014	-1.758104
H	-4.278513	-2.286066	-1.459664
H	-3.625885	-0.810194	-1.126042
H	3.169645	2.019303	0.669640
H	2.007033	2.580085	1.665221
H	3.148440	3.615739	1.084658

```
   25
Complex 5
 U    -0.000109     0.395880    -0.029734
 O    -0.001889     0.479795    -1.800296
 N     0.002409     3.075830     0.099583
 N    -2.378330     1.325373    -0.000006
 N     1.477800    -1.669863    -0.095088
 H    -2.629360     1.857664    -0.831467
 H    -3.114065     0.563816     0.036099
 H    -2.598459     1.909303     0.804897
 H     1.357487    -2.222316    -0.942048
 H     2.510881    -1.462667    -0.055768
 H     1.317405    -2.300027     0.688587
 O     0.001771     0.370341     1.742253
 N     2.378505     1.325119    -0.005163
 N    -1.478178    -1.669814    -0.091346
 H     2.599890     1.911995     0.797236
 H     3.113949     0.563375     0.033198
 H     2.629119     1.854249    -0.838762
 H    -1.318475    -2.298044     0.694027
 H    -2.511295    -1.462447    -0.053521
 H    -1.357253    -2.224386    -0.936830
Br     4.618821    -0.957299     0.058215
Br    -4.619242    -0.956715     0.057362
 H    -0.818688     3.502787    -0.320944
 H     0.808917     3.500470    -0.350537
 H     0.020238     3.368146     1.074653
```

```
   25
Complex 5'
 U     0.015797    -0.165110     0.092362
 O    -0.447750    -1.036335    -1.385454
 N     0.821524    -2.521549     0.981175
Br     2.836418    -0.491710    -0.528663
Br    -2.360893     1.460190    -0.099869
 O     0.462189     0.589601     1.637397
 N    -1.901390    -1.374936     1.384750
 N     0.721343     1.903300    -1.232861
 H    -2.407881    -0.640746     1.873309
 H    -2.543005    -1.753208     0.666030
 H    -1.688402    -2.104174     2.058458
 H    -0.085203     2.460428    -1.499777
 H     1.339635     2.464756    -0.623121
 H     1.246214     1.654750    -2.066276
 N    -3.446695    -1.875369    -1.077173
 N     2.547733     2.863258     0.883952
 H     0.233564    -3.311390     0.731433
 H     1.000630    -2.554337     1.980855
 H     1.719067    -2.626458     0.509962
 H    -2.687912    -2.016964    -1.738697
 H    -4.255552    -2.393826    -1.403685
 H    -3.669669    -0.882103    -1.115400
 H     3.200552     2.098086     0.729003
 H     1.982305     2.604198     1.687657
 H     3.078268     3.694828     1.120757
```

References for the ESI:

[1] a) A. D. Becke, *J. Chem. Phys.* **1993**, *98*, 5648-5652; b) C. Lee, W. Yang and R. G. Parr, *Phys. Rev. B* **1988**, *37*, 785-789.
[2] S. Grimme, S. Ehrlich and L. Goerigk, *J. Comput. Chem.* **2011**, *32*, 1456–1465.
[3] W. Küchle, M. Dolg, H. Stoll and H. Preuss, *J. Chem. Phys.* **1994**, *100*, 7535-7542.
[4] R. Krishnan, J. S. Binkley, R. Seeger and J. A. Pople, *J. Chem. Phys.* **1980**, *72*, 650-654.
[5] P. Woidy, M. Bühl and F. Kraus, *Dalton Trans.* **2015**, *44*, 7332-7337.
[6] a) T. H. Dunning, *J. Chem. Phys.* **1989**, *90*, 1007-1023; b) R. A. Kendall, T. H. Dunning and R. J. Harrison, *J. Chem. Phys.* **1992**, *96*, 6796-6806.
[7] J.-D. Chai and M. Head-Gordon, *J. Chem. Phys.* **2008**, *128*, 084106.
[8] C. Adamo and V. Barone, *J. Chem. Phys.* **1999**, *110*, 6158-6170.
[9] a) J. P. Perdew, in Electronic Structure of Solids '91, Ed. P. Ziesche and H. Eschrig (Akademie Verlag, Berlin, 1991) 11; b) J. P. Perdew, J. A. Chevary, S. H. Vosko, K. A. Jackson, M. R. Pederson, D. J. Singh and C. Fiolhais, *Phys. Rev. B* **1992**, *46*, 6671-6687; c) J. P. Perdew, J. A. Chevary, S. H. Vosko, K. A. Jackson, M. R. Pederson, D. J. Singh and C. Fiolhais, *Phys. Rev. B* **1993**, *48*, 4978-4978; d) J. P. Perdew, K. Burke and Y. Wang, *Phys. Rev. B* **1996**, *54*, 16533-16539; e) K. Burke, J. P. Perdew, and Y. Wang, in Electronic Density Functional Theory: Recent Progress and New Directions, Ed. J. F. Dobson, G. Vignale, and M. P. Das (Plenum, **1998**).
[10] A. D. Becke, *Phys. Rev. A* **1988**, *38*, 3098.
[11] a) J. P. Perdew, *Phys. Rev. B* **1986**, *34*, 7406; b) J. P. Perdew, *Phys. Rev. B* **1986**, *33*, 8822.
[12] S. Grimme, *J. Comput. Chem.* **2006**, *27*, 1787-1799.
[13] Y. Zhao, N. E. Schultz and D. G. Truhlar, *J. Chem. Theory Comput.* **2006**, *2*, 364-382.
[14] Y. Zhao and D. G. Truhlar, *Theor. Chem. Acc.* **2008**, *120*, 215-241.
[15] Y. Zhao and D. G. Truhlar, *J. Chem. Phys.* **2006**, *125*, 194101-194118.
[16] S. F. Boys and F. Bernardi, *Mol. Phys.* **1970**, *19*, 553-566.
[17] a) E. Cancès, B. Mennucci and J. Tomasi, *J. Chem. Phys.* **1997**, *107*, 3032-3041; b) E. Cancès and B. Mennucci, *J. Math. Chem.* **1998**, *23*, 309-326; c) B. Mennucci, E. Cancès and J. Tomasi, *J. Phys. Chem. B* **1997**, *101*, 10506-10517; d) G. Scalmani and M. J. Frisch, *J. Chem. Phys.* **2010**, *132*, 114110.
[18] a) V. Barone and M. Cossi, *J. Phys. Chem. A* **1998**, *102*, 1995-2001; b) C. Maurizio, R. Nadia, S. Giovanni and B. Vincenzo, *J. Comput. Chem.* **2003**, *24*, 669-681.
[19] J. B. Foresman, T. A. Keith, K. B. Wiberg, J. Snoonian and M. J. Frisch, *J. Phys. Chem.* **1996**, *100*, 16098-16104.
[20] A. V. Marenich, C. J. Cramer and D. G. Truhlar, *J. Phys. Chem. B* **2009**, *113*, 6378-6396.
[21] Gaussian 09, Revision D.01, M. J. Frisch, G. W. Trucks, H. B. Schlegel, G. E. Scuseria, M. A. Robb, J. R. Cheeseman, G. Scalmani, V. Barone, B. Mennucci, G. A. Petersson, H. Nakatsuji, M. Caricato, X. Li, H. P. Hratchian, A. F. Izmaylov, J. Bloino, G. Zheng, J. L. Sonnenberg, M. Hada, M. Ehara, K. Toyota, R. Fukuda, J. Hasegawa, M. Ishida, T. Nakajima, Y. Honda, O. Kitao, H. Nakai, T. Vreven, J. A. Montgomery, Jr., J. E. Peralta, F. Ogliaro, M. Bearpark, J. J. Heyd, E. Brothers, K. N. Kudin, V. N. Staroverov, T. Keith, R. Kobayashi, J. Normand, K. Raghavachari, A. Rendell, J. C. Burant, S. S. Iyengar, J. Tomasi, M. Cossi, N. Rega, J. M. Millam, M. Klene, J. E. Knox, J. B. Cross, V. Bakken, C. Adamo, J. Jaramillo, R. Gomperts, R. E. Stratmann, O. Yazyev, A. J. Austin, R. Cammi, C. Pomelli, J. W. Ochterski, R. L. Martin, K. Morokuma, V. G. Zakrzewski, G. A. Voth, P. Salvador, J. J. Dannenberg, S. Dapprich, A. D. Daniels, O. Farkas, J. B. Foresman, J. V. Ortiz, J. Cioslowski, and D. J. Fox, Gaussian, Inc., Wallingford CT, **2013**.
[22] A. Klamt and G. Schüürmann, *J. Chem. Soc. Perkin Trans. 2* **1993**, *5*, 799 - 805.

[23] TURBOMOLE V6.4 2012, a development of University of Karlsruhe and Forschungszentrum Karlsruhe GmbH, 1989-2007, TURBOMOLE GmbH, since 2007; available from http://www.turbomole.com.
[24] A. K. Rappe, C. J. Casewit, K. S. Colwell, W. A. Goddard and W. M. Skiff, *J. Am. Chem. Soc.* **1992**, *114*, 10024-10035.
[25] A. Klamt and V. Jonas, *J. Chem. Phys.* **1996**, *105*, 9972-9981.
[26] Haynes, W.M. (ed.). CRC Handbook of Chemistry and Physics. 95th Edition. CRC Press LLC, Boca Raton: FL 2014-2015, p. 4-137
[27] M. H. Abraham, *J. Phys. Org. Chem.* **1993**, *6*, 660-684.
[28] Weast, R.C. (ed.) Handbook of Chemistry and Physics, 68th ed. Boca Raton, Florida: CRC Press Inc., 1987-1988., p. F-35
[29] a) R. Car and M. Parrinello, *Phys. Rev. Lett.* **1985**, *55*, 2471; b) CPMD Version 3.15.1, Copyright IBM Corp. 1990–2006, Copyright MPI für Festkörperforschung Stuttgart, **1997–2001**
[30] N. Troullier and J. L. Martins, *Phys. Rev. B* **1991**, *43*, 1993.
[31] L. Kleinman and D. M. Bylander, *Phys. Rev. Lett.* **1982**, *48*, 1425.
[32] Sprik, M.; Ciccotti, G. *J. Chem. Phys.* **1998**, *109*, 7737-7744, and references cited therein.